Single Amino Acid Substitutions in Puroindoline-b Mutants Influence Lipid Binding Properties†

Luke A. Clifton, Mitaben D. Lad, Rebecca J. Green, and Richard A. Frazier*

School of Chemistry, Food Biosciences and Pharmacy, University of Reading, PO Box 226, Whiteknights, Reading RG6 6AP, United Kingdom

Received October 21, 2006; Revised Manuscript Received December 19, 2006

ABSTRACT: External reflectance Fourier transform infrared (ER-FTIR) spectroscopy and surface pressure measurements have been used to characterize the interaction of wild-type puroindoline-b (Pin-b) and two mutant forms featuring single residue substitutions—namely, Gly-46 to Ser-46 (Pin-bH) and Trp-44 to Arg-44 (Pin-bS)—with condensed-phase monolayers of zwitterionic (L-α-dipalmitoylphosphatidylcholine, DPPC) and anionic (L-α-dipalmitoylphosphatidyl-*dl*-glycerol, DPPG) phospholipids. The interaction with anionic DPPG monolayers, monitored by surface pressure isotherms, was influenced significantly by mutations in Pin-b ($p < 0.05$); wild-type Pin-b showed the highest surface pressure change of 10.6 ± 1.0 mN m^{-1}, followed by Pin-bH (7.9 ± 1.6 mN m^{-1}) and Pin-bS (6.3 ± 1.0 mN m^{-1}), and the surface pressure isotherm kinetics were also different in each case. Integrated Amide I peak areas from corresponding ER-FTIR spectra confirmed the differences in adsorption kinetics, but also showed that differences in adsorbed amount were less significant, suggesting that mutations influence the degree of penetration into DPPG films. All Pin-b types showed evidence of interaction with DPPC films, detected as changes in surface pressure (5.6 ± 1.1 mN m^{-1}); however, no protein peaks were detected in the ER-FTIR spectra, which indicated that the interaction was via penetration with limited adsorption at the lipid/water interface. The expression of Pin-b mutants is linked to wheat endosperm hardness; therefore, the data presented here suggest that the lipid binding properties may be pivotal within the mechanism for this quality trait. In addition, the data suggest antimicrobial activities of Pin-b mutants would be lower than those of the wild-type Pin-b, because of decreased selectivity toward anionic phospholipids.

Puroindolines are basic, water-soluble proteins that were first identified in wheat (var. *Triticum aestivum*) (*1*, *2*), although homologous proteins have now been found in rye, barley, and oats (*3*, *4*). They exist as two isoforms, puroindoline-a (Pin-a)[1] and puroindoline-b (Pin-b), which exhibit 55% homology in their sequence, and both share lipid binding properties that are attributed to a Trp-rich structural loop enclosed by a disulfide bond. This loop is a unique feature of the puroindolines and features a domain containing five Trp residues in Pin-a in the sequence Trp-Arg-Trp-Trp-Lys-Trp-Trp-Lys, which is truncated to three Trp residues in Pin-b in the sequence Trp-Pro-Thr-Lys-Trp-Trp-Lys. The puroindolines have attracted particular interest for their role in determining wheat endosperm texture (*5*−*7*), which is an important end-use quality parameter, and for their potential antimicrobial (notably antifungal) activity (*1*, *8*−*10*).

A structural model of the puroindolines has been proposed based on primary and secondary structure similarities between the puroindolines and nonspecific lipid transport proteins (ns-LTP) (*11*−*13*). In this model, the generic puroindoline protein contains a hydrophobic "head", consisting of the Trp-rich domain and another smaller Phe-rich domain, which is also truncated in Pin-b. The precise biological function of the puroindolines, although unknown, seems to be related to this amphiphilic structure and the associated lipid binding properties. In previous studies, between four and five lipid binding sites have been found on Pin-a, and both Pin-a and Pin-b have also been shown to bind preferentially to anionic phospholipids (*14*, *15*), although they do also interact with zwitterionic phospholipids and glycolipids.

The gene coding the puroindolines in hexaploid wheat is linked to the *Hardness* locus (*Ha*) on the short arm of chromosome 5D (*16*, *17*), which has been shown to control endosperm texture. Endosperm texture is important for the milling quality of wheat and makes it suitable for a particular end use; hard milling wheat is more suitable for bread, whereas soft milling wheat is suitable for cakes and biscuits. The wild-type wheat is soft textured and hard wheat varieties contain either null forms or mutated forms of the genes controlling the expression of Pin-a and Pin-b. This was first noted by Giroux and Morris (*18*), who discovered a Gly-46 to Ser-46 point mutation on the Pin-b gene (*Pinb-D1b*) of a

* To whom correspondence should be addressed. Tel.: +44 118 3788709. Fax: +44 118 9310080. E-mail: r.a.frazier@reading.ac.uk.

† This work was supported by the U.K. Biotechnology and Biological Sciences Research Council (Studentship BBSSA200411018).

[1] Abbreviations: CMC, carboxymethylcellulose; DPPC, L-α-dipalmitoylphosphatidylcholine; DPPG, dipalmitoylphosphatidyl-*dl*-glycerol; ER-FTIR, external reflection Fourier transform infrared; HPLC, high-performance liquid chromatography; Pin-a, Puroindoline-a; Pin-b, Puroindoline-b; PTFE, polytetrafluoroethylene; SDS-PAGE, sodium dodecyl sulfate−polyacrylamide gel electrophoresis; UHQ, ultrahigh quality.

10.1021/bi062190h CCC: $37.00
Published on Web 02/03/2007

	29																		48
Pin-b	C	F	T	M	K	D	F	P	V	T	W	P	T	K	W	W	K	G	G	C
Pin-bH	C	F	T	M	K	D	F	P	V	T	W	P	T	K	W	W	K	**S**	G	C
Pin-bS	C	F	T	M	K	D	F	P	V	T	W	P	T	K	W	**R**	K	G	G	C

FIGURE 1: Sequences of the Trp-rich loop for the wild-type Pin-b and the mutants Pin-bH (Gly-46 to Ser-46) and Pin-bS (Trp-44 to Arg-44). The loop is formed by a disulfide bond between Cys-29 and Cys-48.

hard variety, which occurred within the 18-residue Trp-rich loop (enclosed by a disulfide bond between Cys-29 and Cys-48 in Pin-b). They later discovered that this mutation occurred in a series of hard wheat types (*19*). Further altered alleles of the puroindolines were then found, either encoding mutation near or within the Trp-rich loop for Pin-b (Lue-60 to Pro-60 and Trp-44 to Arg-44 point mutations) or stopping the synthesis of Pin-a or Pin-b altogether (*20*, *21*). These mutations in the puroindoline genes seem to be fundamental to hard wheat texture.

Despite this well-documented genetic evidence for the role of puroindolines in endosperm texture, the precise biochemical mechanism remains unclear. In hard wheat varieties, strong adhesion is observed between starch granules and the surrounding protein matrix within the endosperm, whereas, in soft wheat varieties, the adhesion is weak. In localization studies of the mature starchy endosperm, puroindolines have been shown to be present in the protein matrix and, critically, at the interface between this matrix and starch granules (*5*, *22*). It has been suggested that the presence of puroindolines on the surface of starch granules could be lipid mediated (*23*), because this interface has been shown to contain lipid membrane remnants (*24*). However, conclusive evidence does not exist to support this hypothesis or to suggest how genetic mutations might exert an influence.

The objective of this study was to investigate the interaction of three different Pin-b types with condensed phase anionic and zwitterionic lipid films, with the objective to determine whether point mutations influence lipid binding properties. The proteins studied were the wild-type Pin-b, Pin-b containing the Gly-46 to Ser-46 mutation (denoted Pin-bH, as it was obtained from the Hereward hard wheat variety), and Pin-b containing a Trp-44 to Arg-44 mutation (denoted here as Pin-bS, as it was obtained from the Soissons hard wheat variety). The positions of the mutations within the sequence of the 18-peptide Trp-rich loop are highlighted in Figure 1. Surface pressure measurements and external reflection Fourier transform infrared (ER-FTIR) spectroscopy were used for analysis. ER-FTIR spectroscopy is performed at the air/water interface and is especially suited for the study of protein−lipid interactions, because it allows for determination of the secondary structure of the protein and conformation of lipid acyl chains during the interaction.

MATERIALS AND METHODS

Materials. L-α-Dipalmitoylphosphatidylcholine (DPPC, synthetic purity >99%) and L-α-dipalmitoylphosphatidyl-*dl*-glycerol (DPPG, synthetic purity >99%) were purchased from Avanti Polar Lipids (Alabaster, AL) and were used without further purification. Stock solutions (1 g dm^{-3}) of DPPC and DPPG were prepared in HPLC-grade chloroform (Sigma-Aldrich, Dorset, U.K.) and stored at room temperature, with 1:2 dilutions of these solutions being used experimentally. Pin-b proteins were extracted from wheat flour and purified using Triton X-114 phase partitioning and chromatographic techniques, as described in the next section. All other chemicals were obtained from Sigma−Aldrich and were of the highest purity available.

For surface pressure measurements, protein solutions (0.1 g dm^{-3}) were prepared in phosphate buffer solution at pH 7 (I = 0.02 M) using UHQ-grade water. For ER-FTIR spectroscopy, protein stock solutions (0.1 g dm^{-3}) were prepared in D_2O phosphate buffer solution at pH 7 (I = 0.02 M). Solutions used in ER-FTIR spectroscopy experiments were prepared 24 h in advance, to allow for sufficient H−D exchange (*25*).

Pin-b Purification. Wild-type Pin-b, Pin-b with a Gly-46 to Ser-46 mutation (Pin-bH), and Pin-b with a Trp-44 to Arg-44 mutation (Pin-bS) were extracted and purified from the wheat varieties Claire, Hereward, and Soissons, respectively. The procedure used is detailed below and was that described by Day (*26*) as a modification of the procedure first reported by Kooijman et al. (*27*).

Wheat flour (480 g) was mixed with a PEK buffer (0.05 M sodium phosphate, pH 7.6, 5 mM ethylenediaminetetraacetic acid, 0.05 M KCl; 2.4 dm^3) at 4 °C for 1 h. After the pellet was subjected to centrifuging (3 500×*g*, 10 min), it was extracted with 4% (v/v) Triton X-114 in a PEK buffer (1.2 dm^3) at 4 °C for 2 h. After centrifugation (13 000×*g*, 10 min), the pellet was discarded and the pH of the supernatant was adjusted to 4.5 with glacial acetic acid. Carboxymethylcellulose (CMC, 24 g) was added to the Triton X-114 solution, and this mixture was stirred at 4 °C for 12 h. After centrifugation (13 000×*g*, 10 min), the pellet was washed with 0.05 M acetic acid solution (800 cm^3, two times). The CMC-bound proteins were then eluted with 1 M NaCl in 0.05 M acetic acid (160 cm^3) at 4 °C for 1 h. Following filtration to remove the CMC, 28 g of NaCl was added to the filtrate. After mixing for 1 h and centrifugation (13 000×*g*, 10 min), the pellet was dissolved in 0.05 M acetic acid (40 cm^3) and dialyzed against 0.05 M acetic acid (2 × 5 dm^3, 48 h), then lyophilized.

Cation exchange chromatography was then conducted, using a preparative Mono-S HR 16/10 column (Pharmacia Biotech UK, Buckinghamshire, U.K.) and a BioCad Sprint perfusion chromatography system (Global Medical Instruments, Minneapolis, MN). The sample was prepared by dissolving lyophilized crude protein (60 mg) in 2.5 cm^3 of 0.05 M ammonium acetate, pH 5.5, 25% (v/v) acetonitrile, heating at 30 °C for 30 min prior to centrifugation (3500×*g*, 10 min), and subjecting it to filtration.

The CMC-bound protein fraction was eluted over a gradient of 0.05−1 M ammonium acetate, pH 5.5, 25% (v/v) acetonitrile. The flow rate was constant at 3 cm^3 min^{-1}, and the absorbance was monitored at a wavelength of 280 nm. The Pin-b fraction was eluted at an ammonium acetate concentration of 0.6 M. Fractions were dialyzed against deionized water (5 dm^3, for 48 h, refreshed every 24 h) and lyophilized. The purity and identity of the lyophilized Pin-b fraction was confirmed using SDS-PAGE (*28*) and capillary electrophoresis (*26*). The proteins were stored at −20 °C until use.

Surface Pressure Measurements. Surface pressure measurements were performed using a polytetrafluoroethylene (PTFE) Langmuir trough (model 611, Nima Technology Ltd,

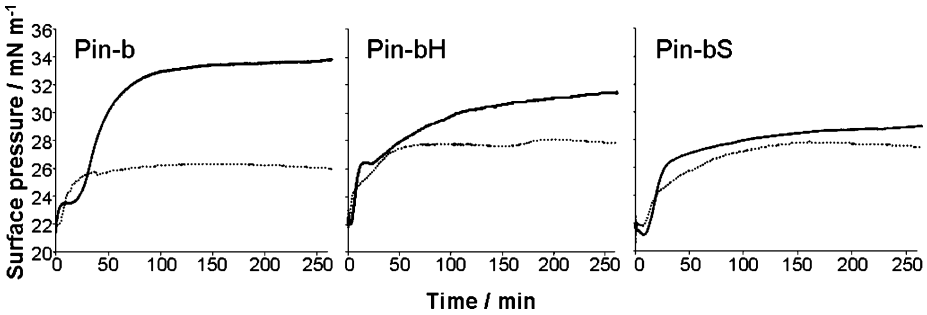

FIGURE 2: Surface pressure isotherms for the interaction of Pin-b, Pin-bH, and Pin-bS with DPPG monolayers (solid lines) and DPPC monolayers (dotted lines) at the air/water interface.

Coventry, U.K.) that was equipped with barriers for the preparation of compressed lipid layers, and the surface pressure was monitored using a filter paper Wilhelmy plate surface pressure sensor. A new Wilhemy plate was used for each experiment. To create lipid monolayers at the air/water interface, the trough was filled with 80 cm^3 of 0.02 M phosphate buffer (pH 7). Twenty microliters of lipid solution (0.5 g dm^{-3}) was spread at the air/water interface and compressed to a surface pressure of 22 mN m^{-1}. The compressed lipid films were monitored via measurements of the pressure (π) versus time to check the stability of these films. A 0.5 cm^3 sample of the appropriate 0.1 g dm^{-3} puroindoline solution was then added to the aqueous subphase to give a final concentration of 6 μg cm^{-3} (0.46 μM). Changes in the surface pressure, as a result of puroindoline adsorption, were monitored by plotting the surface pressure versus time, keeping the layer compression (area) constant for a total of 260 min.

FTIR Spectroscopy. ER-FTIR spectra were recorded using a ThermoNicolet Nexus instrument (Madison, WI) that was fitted with a monolayer/grazing angle accessory (Specac 19650 series, Kent, U.K.), a mercury cadmium telluride detector, and an air dryer to purge the instrument of water vapor and carbon dioxide. Lipid−protein interactions were analyzed by external reflectance using the method described by Lad et al. (*29*). The monolayer/grazing angle accessory was equipped with a PTFE trough (94 mm × 22 mm × 5 mm) and a barrier for the preparation of compressed lipid layers, which were aligned at an angle of incidence of 45° to the air/water interface. All spectra were recorded at a resolution of 4 cm^{-1}, where 256 interferograms were collected, co-added, and ratioed against the buffer.

During each experiment, 7.5 cm^3 of D_2O phosphate buffer ($I = 0.02$ M, pH 7) was placed in the trough and the single-beam background spectra were recorded after time was added for the sample chamber to purge H_2O and CO_2. After recording the background spectra, 5 μL of a 0.5 g dm^{-3} lipid solution was added to the buffer surface and then compressed to the predefined 22 mN m^{-1} condensed-phase position that was determined using surface pressure measurements. Sample scans were taken to ensure the stability of the lipid film and checked via the observation of the symmetric and asymmetric CH_2 stretching of the lipid chain at 2854−2850 cm^{-1} and 2924−2916 cm^{-1}, respectively. A 0.5 cm^3 sample of a 0.1 g dm^{-3} protein solution was then added to the aqueous subphase without disturbing the lipid monolayer, to give a final concentration of 6.25 μg cm^{-3} (0.48 μM). Spectra were continuously taken from the moment of protein introduction to the system for the initial 15 min of the experiment, followed by 1 spectrum every 15 min thereafter. Spectra were recorded for a total of 260 min. The interaction of the protein with the lipid monolayer was observed by monitoring the Amide I band at ~1650 cm^{-1} and the lipid acyl chain vibrations (~2920 and 2850 cm^{-1}). Protein adsorption to the bare air/water interface was conducted using the aforementioned method without the presence of the lipid monolayer.

All spectra were corrected for complete removal of the H_2O and HOD peaks from the amide spectral region. To correct for water vapor, H_2O and HOD spectra were scaled and subtracted against each protein spectrum. The degree of subtraction was dependent on the absorption time and H/D exchange. The HOD spectra were recorded during the purge of the air/liquid sample area prior to the addition of the lipid film (*29*). No further processing was performed.

FTIR transmission spectra of protein solutions were recorded using a deuterium triglyceride sulfate detector. Protein solutions were made to a concentration of 2 mg cm^{-3} (154 μmol dm^{-3}) in D_2O phosphate buffer ($I = 0.02$ M, pH 7) and placed in a Specac Omni liquid cell (Specac, Kent, U.K.) fitted with CaF_2 windows and a Mylar spacer to give a path length of 6 μm. Spectra were collected as interferograms at 4 cm^{-1} resolution, where 64 interferrograms were collected, co-added, and ratioed against a background spectrum of the buffer solution.

The Fourier self-deconvolution process was performed on the Amide I peaks of the protein spectra using the instrument software. The bandwidth was maintained constant for each spectrum. The resulting bands are not "real" and, therefore, are used solely as a qualitative comparison tool.

Data Analysis. Statistical analysis was performed using two-tailed Student's t-tests to determine significant differences between means at an acceptable level of error ($\alpha = 0.05$). Differences were considered significant at a probability of error (p) of $p < \alpha$. Analyses were performed at least in triplicate.

RESULTS

Surface Pressure Measurements. Figure 2 shows the surface pressure isotherms (surface pressure versus time) upon the addition of wild-type Pin-b, Pin-bS, and Pin-bH into the aqueous subphase, in the presence of condensed DPPC and DPPG monolayers at the air/water interface. The interaction of the three Pin-b proteins with a DPPC monolayer led to similar surface pressure increases, which all were within the range of 5.6 ± 1.1 mN m^{-1}. The surface pressure changes for each protein are given in Table 1, and, although there is some variation in the data for interaction with DPPC

Table 1: Surface Pressure Changes for Puroindoline Interaction with Lipid and Air/Water Interfaces[a]

	Surface Pressure Change (mN m^{-1})		
Pin-b mutant	DPPC	DPPG	air/water
wild-type Pin-b	4.3 ± 0.1^{a1}	10.6 ± 1.0^{b1}	12.8 ± 0.1^{1}
Pin-bH	6.5 ± 0.4^{a2}	7.9 ± 1.6^{a2}	12.4 ± 0.1^{1}
Pin-bS	5.5 ± 0.4^{a2}	6.3 ± 1.0^{a2}	11.5 ± 0.3^{2}

[a] Different superscripted letters denote significant differences in a row ($p < 0.05$). Different superscripted numbers denote significant differences in a column ($p < 0.05$).

monolayers, this is only statistically significant ($p < 0.05$) in that Pin-bH and Pin-bS gave greater surface pressure changes than the wild-type Pin-b. However, it should be noted that the difference represents a change only of 1.2−2.2 mN m^{-1}.

With DPPG, there was evidence of a stronger interaction for all three Pin-b types, although the overall surface pressure change and kinetics were different for each protein. Wild-type Pin-b gave the highest overall surface pressure change of 10.6 ± 1.0 mN m^{-1} after 4 h, followed by Pin-bH (with a corresponding surface pressure change of 7.9 ± 1.6 mN m^{-1}) and Pin-bS (with a surface pressure change of 6.3 ± 1.0 mN m^{-1}). In terms of the surface pressure kinetics, inspection of Figure 2 reveals that both wild-type Pin-b and Pin-bH displayed clear two-step isotherms, whereas Pin-bS had a one-step isotherm, following an initial induction period. Induction periods are a common feature of surface pressure isotherms and do not necessarily indicate an absence of adsorption, because surface pressure measurements are sensitive to changes in surface tension that are caused by the adsorbing species rather than adsorbed amount. Indeed, it has been shown previously that, for the adsorption of a protein to the air/water interface, 50% molecular surface coverage may be required before a change in surface pressure is detected (*30*). In the presence of a lipid layer at the interface, it is likely that surface pressure measurements are more sensitive to penetration of the existing interfacial monolayer, rather than adsorption to it (i.e., the formation of a second adsorbed layer) (*29*).

External Reflectance FTIR Spectra. Upon the addition of the Pin-b proteins to the buffer subphase of a condensed-phase DPPC monolayer, no Amide I band was observed for any of the proteins and no significant change in the lipid acyl chain spectra was detected (data not shown). This seems to contradict the surface pressure measurements; however, note that, in the absence of bulk surface adsorption, ER-FTIR spectra will be relatively insensitive to penetration by a small number of protein molecules, which could lead to significant surface pressure changes, as discussed previously.

Figure 3 shows the lipid acyl and lipid carbonyl/Amide I band spectral regions during wild-type Pin-b, Pin-bH, and Pin-bS interaction with DPPG. All three sets of spectra show the gradual appearance of an Amide I band at ~1641 cm^{-1}, corresponding to protein adsorption, while showing no changes to the lipid spectra. In addition, it was noted that the protein structure that was indicated by deconvolution of the Amide I band was the same for each of the Pin-b types.

Figure 4 shows the corresponding Amide I peak area-versus-time plots for the adsorption of each of the Pin-b proteins. All three proteins had adsorption profiles from ER-FTIR integrated spectra that were similar to those observed by surface pressure measurements. However, it was noteworthy that the final adsorbed amounts were similar for each protein, which does not agree with the differences in surface pressure changes that were observed. This suggests that the surface pressure measurements were influenced more by lipid layer penetration than by surface adsorption alone, as has been discussed earlier.

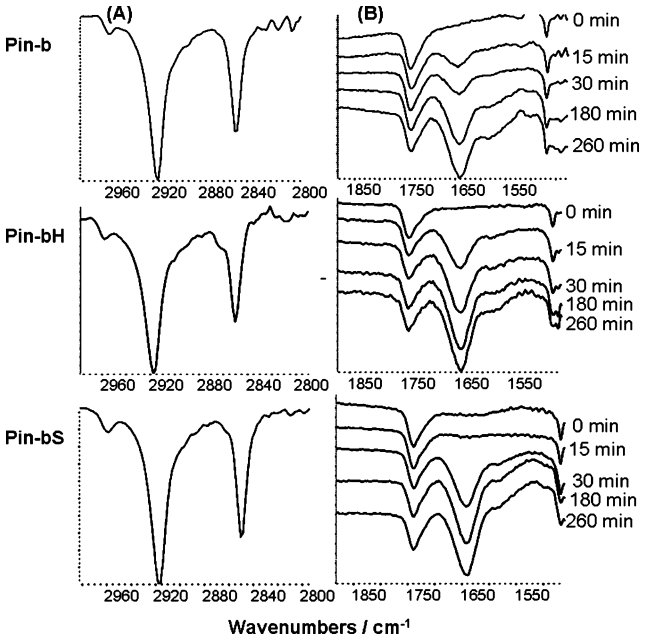

FIGURE 3: ER-FTIR spectra of the (A) lipid acyl region and (B) amide region for the interaction of Pin-b, Pin-bH, and Pin-bS with DPPG monolayers at the air/water interface. The lipid acyl region (A) includes peaks for the CH_3 stretch (2960 cm^{-1}) and CH_2 symmetric and asymmetric stretches (2850 and 2920 cm^{-1}, respectively). The amide region (B) includes a CO stretch at 1750 cm^{-1}, which is due to the head group carbonyl of DPPG, and the gradual appearance of an Amide I peak at 1650 cm^{-1}, which is due to protein adsorption.

Adsorption to Bare Air/Water Interface. To assess the influence of mutations on surface activity, ER-FTIR spectra and surface pressure isotherms were recorded during adsorption to the bare air/water interface. Figure 5 shows integrated Amide I peak areas from two replicates of these experiments, which, in all cases, appeared at ~1644 cm^{-1}. Table 1 includes the surface pressure changes recorded from the corresponding surface pressure isotherms (not shown). From these data, it can be observed that the surface activities of wild-type Pin-b and Pin-bH are similar, whereas Pin-bS exhibits a significantly lower surface activity ($p < 0.05$).

Deconvolution of Amide I FTIR Transmission and ER-FTIR Spectra. Protein Amide I peaks for each protein in solution and adsorbed to the air/water interface, both with and without the presence of a DPPG monolayer, are shown in Figure 6. The secondary structures of each of the proteins in solution (pH 7) are shown to be very similar, by the shape of the Amide I peaks (see Figure 6A). Indeed, the protein structure of the three proteins remain comparable when adsorbed at an air/water or DPPG interface (Figure 6B), suggesting that the mutations have little to no effect on the secondary structural elements of the protein structure. However, a difference is observed regarding the adsorbed structure of the proteins at the different interfaces, with differing relative amounts of helix and sheet contributing to

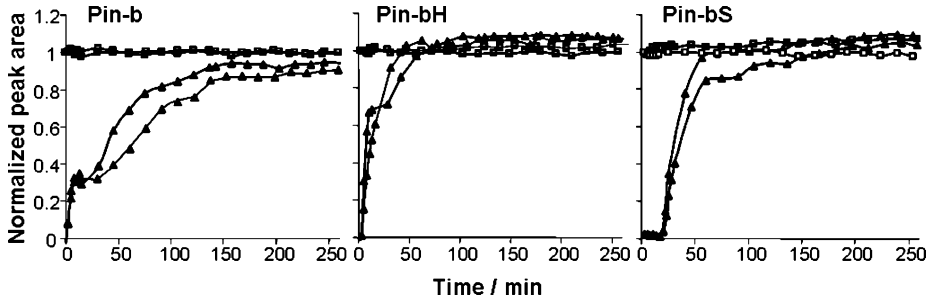

FIGURE 4: Integrated peak areas of the ([□]) CH_2 asymmetric stretch (2920 cm^{-1}) and (▲) Amide I peak (1650 cm^{-1}) from ER-FTIR spectra recorded during the interaction of Pin-b, Pin-bH, and Pin-bS with DPPG monolayers at the air/water interface. The peak areas were normalized against the area of the CH_2 asymmetric stretch for DPPG prior to the introduction of protein to the aqueous subphase.

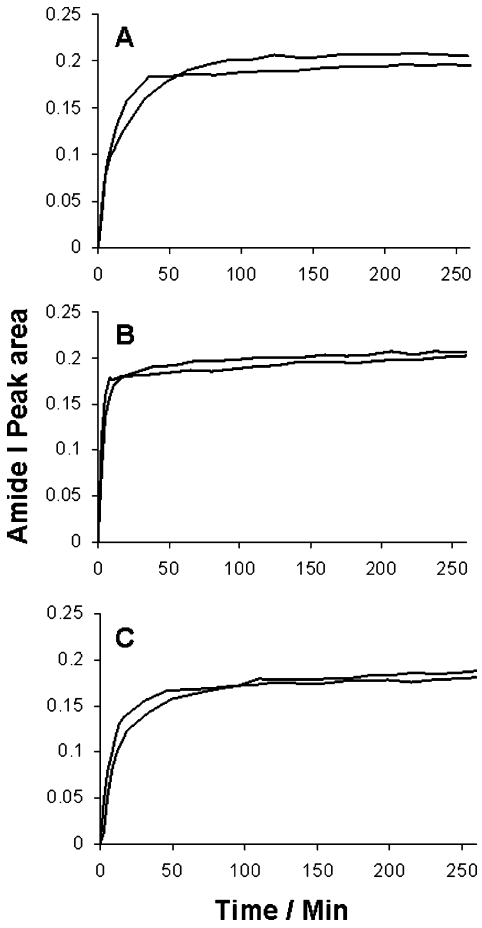

FIGURE 5: Integrated Amide I peak areas from ER-FTIR spectra recorded during the adsorption of (A) Pin-b, (B) Pin-bH, and (C) Pin-bS at the air/water interface.

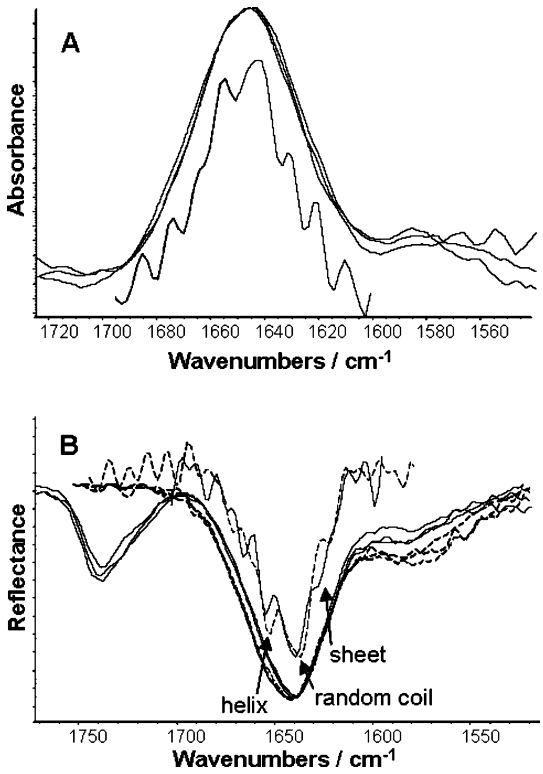

FIGURE 6: Amide I regions and deconvoluted Amide I peaks from (A) transmission FTIR spectra of Pin-b, Pin-bH, and Pin-bS in solution at pH 7, and (B) ER-FTIR spectra of Pin-b, Pin-bH, and Pin-bS adsorbed at the air/water (dashed lines) and DPPG lipid (solid lines) interfaces.

the Amide I peak. This seems to suggest a relative loss of helical structure toward β-sheet structure when the protein is in contact with the lipid layer.

DISCUSSION

The data from surface pressure measurements and ER-FTIR spectroscopy reveal a distinct difference in the lipid interactions of the Pin-b mutants, in comparison to the wild-type Pin-b. Wild-type Pin-b exhibits selectivity in its adsorption/penetration, interacting more strongly with the anionic DPPG than with the zwitterionic DPPC monolayers, in terms of both monolayer penetration and amount adsorbed. This selectivity is not so apparent in the adsorption/penetration of both Pin-b mutants, which did not differ significantly in their interaction with the two lipid monolayers as measured by surface pressure changes. However, ER-FTIR spectroscopy did reveal a significant difference in the adsorbed amount, which suggests that the difference in the interactions between DPPC and DPPG is predominantly due to the relative electrostatic interaction with the polar head groups, which leads to adsorption below the lipid layer, in the case of the anionic DPPG.

The interaction with condensed-phase DPPG monolayers produced notable differences between each protein. Based on the assumption that surface pressure measurements are indicative of lipid penetration, the highest degree of penetration was exhibited by the wild-type Pin-b, followed by Pin-bH and Pin-bS with significantly lower penetration. The Pin-bH mutation is a Gly-46 to Ser-46 point mutation. Ser is a more-polar residue, although both residues are uncharged at neutral pH. The difference in polarity of the Trp-rich loop of this mutant to that of the wild-type Pin-b may influence lipid penetration/adsorption; however, this polarity change is minor, in relation to the size of the loop. Therefore, the

main effect of the Gly-46 to Ser-46 mutation is more likely to be a loss of conformational freedom in the Trp-rich loop of the mutant, because of the bulkier Ser side-chain. Gly is known to possess a large amount of rotational freedom around the bonds to its α-carbon, because of its small hydrogen side-chain (*31*), whereas the bulkier side-chains of the other amino acids constrain bond rotation (*32*). In addition, there is the possibility of hydrogen-bonding side-chain interactions between Ser and other polar residues that may influence the conformation of the Trp-rich loop. Therefore, the net reduction of the conformational flexibility of the Trp-rich loop in Pin-bH may hinder lipid layer penetration.

In the case of Pin-bS, the mutation is Trp-44 to Arg-44. This mutation would be expected to have important consequences for the lipid binding properties, because a nonpolar residue is replaced with a basic residue that will carry a positive charge over a wide pH range and is capable of forming multiple hydrogen bonds. Indeed, Pin-bS adsorption to the air/water interface was less than that for the wild-type Pin-b, which implies that Pin-bS is the more polar. More importantly, however, Trp residues are reported to have an important role in the translocation of membrane proteins and peptides (*33*, *34*), thus a reduction in their number within the Trp-rich loop is likely to reduce the propensity for lipid layer penetration. In addition, the basic Arg residue may interact strongly with the anionic head group of DPPG, which may interfere with orientation of the remaining Trp residues, with respect to their ability to form hydrogen bonds with the lipid head group while their hydrophobic rings penetrate to interact with the lipid acyl chains (*34*).

In terms of kinetics, wild-type Pin-b and Pin-bH both exhibited a two-step interaction process with DPPG in surface pressure isotherms and ER-FTIR data, although this was not always evident in ER-FTIR data for Pin-bH (see Figure 4). This process might be associated with initial protein penetration of the lipid monolayer, followed by a secondary aggregation around these penetration points to form aggregated protein bodies within the monolayer, as was observed by Dubriel et al. in studies of Pin-a adsorption to similar monolayers (*35*). Pin-bS did not show this two-step phenomenon in its interaction process and, moreover, exhibited an induction time to interaction; this slower process may be associated with reduced lipid penetration properties because of the loss of a Trp residue. The lack of a second step in the interaction process may imply that aggregation does not occur post-penetration.

From the FTIR transmission and ER-FTIR spectral data, it was noted that no secondary structural differences were observed between any of the Pin-b types, indicating that the Gly-46 to Ser-46 and Trp-44 to Arg-44 mutations cause no changes to post-translational folding of the protein. The solution Amide I band of all three proteins featured the secondary structural characteristics of the wild-type Pin-b reported by Le Bihan et al. (*11*). It was further noted that there were no differences in the spectra of the Pin-b types when adsorbed at the air/water or DPPG interfaces, although there was a shift from helical to sheet structure in the presence of lipids. This implies that if differences in lipid binding properties were associated to protein structure, then this was due to random coil elements, which would include the Trp-rich loop.

For the interaction of all Pin-b types with DPPC and DPPG, it was noted from ER-FTIR spectra that there was no disruption of the ordering of the lipid acyl chains within the monolayer (*29*). This would have implications for the antimicrobial activity of Pin-b and suggest that it acts by forming pores in lipid membranes, as was also suggested by Charnet et al. for Pin-a and Pin-b (*8*). The selectivity toward anionic phospholipids shown by the wild-type Pin-b suggests antimicrobial selectivity toward bacterial cell membranes (*36*). The lipid interaction characteristics of the Pin-b mutants, including lower penetration and decreased selectivity, would suggest lower antimicrobial activity for these proteins.

The data on the lipid interactions of the Pin-b mutants has demonstrated that the Trp-rich loop can be considered as the primary binding site for this interaction. Furthermore, single amino acid substitutions have been shown to alter the binding properties of the protein, which may have implications for the function of Pin-b in the wheat endosperm. It has been reported that the majority of starch bound lipids in wheat endosperm are polar phospholipids (*37*); therefore, because of their affinity for the lipids demonstrated here and by others, it seems feasible that puroindolines are deposited onto the surface of starch granules via a lipid-mediated mechanism, as was hypothesized by Greenblatt et al. (*23*). The lower penetration of the Pin-b mutants might lead to differences in the amounts deposited, relative to the wild-type Pin-b, which suggests that the puroindolines do have a mechanistic role in endosperm texture and are not merely genetic markers.

ACKNOWLEDGMENT

We thank Campden & Chorleywood Food Research Association for the donation of wheat flour samples, and we thank Dr. Dhan Bhandari and Mr. Doug Smith for their advice on puroindoline purification.

REFERENCES

1. Blochet, J.-E., Chevalier, C., Forest, E., Pebay-Peyroula, E., Gautier, M.-F., Joudrier, P., Pézolet, M., and Marion, D. (1993) Complete amino acid sequence of puroindoline, a new basic and cystine-rich protein with a unique tryptophan-rich domain, isolated from wheat endosperm by Triton X-114 phase partitioning, *FEBS Lett. 329*, 336−340.
2. Gautier, M.-F., Aleman, M.-E., Guirao, A., Marion, D., and Joudrier, P. (1994) *Triticum aestivum* puroindolines, two basic cystine-rich seed proteins: cDNA sequence analysis and developmental gene expression, *Plant Mol. Biol. 25*, 43−57.
3. Darlington, H. F., Tecsi, L., Harris, N., Griggs, D. L., Cantrell, I. C., and Shewry, P. R. (2000) Starch granule associated proteins in barley and wheat, *J. Cereal Sci. 32*, 21−29.
4. Tanchak, M. A., Schernthaner, J. P., Giband, M., and Altosaar, I. (1998) Tryptophanins: isolation and molecular characterization of oat cDNA clones encoding proteins structurally related to puroindoline and wheat grain softness proteins, *Plant Sci. 137*, 173−184.
5. Greenwell, P., and Schofield, J. D. (1986) A starch granule protein associated with endosperm softness in wheat, *Cereal Chem. 63*, 379−380.
6. Jolly, C. J., Rahman, S., Kortt, A. A., and Higgins, T. J. V. (1993) Characterisation of the wheat Mr 15 000 "grain softness protein" and analysis of the relationship between its accumulation in the whole seed and grain softness, *Theor. Appl. Genet. 86*, 589−597.
7. Morris, C. F., Greenblatt, G. A., Bettge, A. D., and Malkawi, H. I. (1994) Isolation and characterization of multiple forms of friabilin, *J. Cereal Sci. 21*, 167−174.

8. Charnet, P., Molle, G., Marion, D., Rousset, M., and Lullien-Pellerin, V. (2003) Puroindolines form ion channels in biological membranes, *Biophys. J. 84*, 2416−2426.
9. Krishnamurthy, K., Balconi, C., Sherwood, J. E., and Giroux, M. J. (2001) Wheat puroindolines enhance fungal disease resistance in transgenic rice, *Mol. Plant−Microbe Interact. 14*, 1255−1260.
10. Faize, M., Sourice, S., Dupuis, F., Parisi, L., Gautier, M. F., and Chevreau, E. (2004) Expression of wheat puroindoline-b reduces scab susceptibility in transgenic apple *(Malus x domestica Borkh.)*, *Plant Sci. 167*, 347−354.
11. Le Bihan, T., Blochet, J.-E., Désormeaux, A., Marion, D., and Pézolet, M. (1996) Determination of the secondary structure and conformation of puroindolines by infrared and Raman spectroscopy, *Biochemistry 35*, 12712−12722.
12. Douliez, J. P., Michon, T., Elmorjani, K., and Marion, D. (2000) Structure, biological and technological functions of lipid transfer proteins and indolines, the major lipid binding proteins from cereal kernels, *J. Cereal Sci. 32*, 1−20.
13. Autran, J. C., Hamer, R. J., Plijter, J. J., and Pogna, N. E. (1997) Exploring and improving the industrial use of wheats, *Cereal Foods World 42*, 216−227.
14. Wilde, P. J., Clark, D. C., and Marion, D. (1993) Influence of competitive adsorption of a lysopalmitoylphosphatidylcholine on the functional properties of puroindoline, a lipid-binding protein isolated from wheat flour, *J. Agric. Food Chem. 41*, 1570−1576.
15. Dubriel, L., Compoint, J.-P., and Marion, D. (1997) Interaction of puroindolines with wheat flour polar lipids determines their foaming properties, *J. Agric. Food Chem. 45*, 108−116.
16. Mattern, P. J., Morris, R., Schmidt, J. W., and Johnson, V. A. (1973) Location of genes for kernal properties in wheat variety 'Cheyenne' using chromosome substitution lines, in *Proceedings of the 4th International Wheat Genetics Symposium*, University of Missouri−Columbia, pp 703−708.
17. Sourdille, P., Perretant, M. R., Charmet, G., Leroy, P., Gautier, M.-F., Joudrier, P., Nelson, J. C., Sorrells, M. E. and Bernard, M. (1996) Linkage between RFLP markers and genes affecting kernel hardness in wheat, *Theor. Appl. Genet. 93*, 580−586.
18. Giroux, M. J., and Morris, C. F. (1997) A glycine to serine change in puroindoline b is associated with wheat grain hardness and low levels of starch-surface friabilin, *Theor. Appl. Genet. 95*, 857−864.
19. Morris, C. F., Lillemo, M., Simeone, M. C., Giroux, M. J., Babb, S. L., and Kidwell, K. K. (2001) Prevalence of puroindoline grain hardness genotypes among historically significant North American spring and winter wheats, *Crop Sci. 41*, 218−228.
20. Giroux, M. J., Talbert, L. E., Habernicht, D. K., Lanning, S., Hemphill, A., and Martin, J. M. (2000) Association of puroindoline sequence type and grain hardness in hard red spring wheat, *Crop Sci. 40*, 370−374.
21. Martin, J. M., Frohberg, R. C., Morris, C. F., Talbert, L. E., and Giroux, M. J. (2001) Milling and bread baking traits associated with puroindoline sequence type in hard red spring wheat, *Crop Sci. 41*, 228−234.
22. Dubreil, L., Gaborit, T., Bouchet, B., Gallant, D. J., Broekaert, W. F., Quillien, L., and Marion, D. (1998) Spatial and temporal distribution of the major isoforms of puroindolines (puroindoline-a and puroindoline-b) and nonspecific lipid transfer protein (ns-LTP1e$_1$) of *Triticum aestivum* seeds. Relationships with their in vitro antifungal properties, *Plant Sci. 138*, 121−135.
23. Greenblatt, G. A., Bettge, A. D., and Morris, C. F. (1995) Relationship between endosperm texture and occurrence of friabilin and bound polar lipids on wheat starch, *Cereal Chem. 72*, 172−176.
24. Al-Saleh, A., Marion, D., and Gallant, D. J. (1986) Microstructure of mealy and vitreous wheat endosperms (*Triticum durum L.*) with special emphasis on location and polymorphic behaviour of lipids, *Food Microstruct. 5*, 131−140.
25. Green, R. J., Hopkinson, I., and Jones, R. A. L. (1999) Unfolding and intermolecular association in globular proteins adsorbed at interfaces, *Langmuir 15*, 5102−5110.
26. Day, L., Bhandari, D. G., Greenwell, P., Leonard, S. A., and Schofield, J. D. (2006) Characterization of wheat puroindoline proteins, *FEBS J. 273*, 5358−5373.
27. Kooijman, M., Orsel, R., Hessing, M., Hamer, R. J., Bekkers, A. C. A. P. A. (1997) Spectroscopic characterisation of the lipid-binding properties of wheat puroindolines, *J. Cereal Sci. 26*, 145−159.
28. Laemmli, U. K., and Favre, M. (1973) Maturation of the head of bacteriophage T4 DNA packaging events, *J. Mol. Biol. 80*, 575−599.
29. Lad, M. D., Birembaut, F., Frazier, R. A., and Green, R. J. (2005) Protein−lipid interactions at the air/water interface, *Phys. Chem. Chem. Phys. 7*, 3478−3485.
30. Tripp, B. C., Magda, J. J., and Andrade, J. D. (1995) Adsorpion of globular proteins at the air/water interface as measured via dynamic surface tension: concentration dependence, mass-transfer considerations, and adsorption kinetics, *J. Colloid Interface Sci. 173*, 16−27.
31. Ramachandran, G. N., and Sasisekharan, V. (1968) Conformation of polypeptides and proteins, *Adv. Protein Chem. 23*, 283−437.
32. Richardson, J. S. (1981) The anatomy and taxonomy of protein structure, *Adv. Protein Chem. 34*, 167−336.
33. Gatineau, E., Toma, F., Montenay-Garestier, T., and Takechi, M. (1987) Role of tyrosine and tryptophan residues in the structure−activity relationships of a cardiotoxin from Naja nigricollis venom, *Biochemistry 26*, 8046−8055.
34. Schiffer, M., Chang, C.-H., and Stevens, F. J. (1992) The functions of tryptophan residues in membrane proteins, *Protein Eng. 5*, 213−214.
35. Dubreil, L., Vié, V., Beaufils, S., Marion, D., and Renault, A. (2003) Aggregation of puroindoline in phospholipid monolayers spread at the air−liquid interface, *Biophys. J. 85*, 2650−2660.
36. Yeaman, M. R., and Yount, N. Y. (2003) Mechanisms of antimicrobial peptide action and resistance, *Pharmacol. Rev. 55*, 27−55.
37. Konopka, I., Rotkiewicz, D., and Tanska, M. (2005) Wheat endosperm hardness. Part II. Relationships to content and composition of flour lipids, *Eur. Food Res. Technol. 220*, 20−24.

BI062190H